



Sterols, free fatty acids, and total fatty acid content in the massive *Porites* spp. corals cultured under different pCO₂ and temperature treatments

Nora S. H. von Xylander^{1,2} · Simon A. Young¹ · Catherine Cole^{2,3} · Terry K. Smith¹ · Nicola Allison²

Received: 28 June 2022 / Accepted: 6 February 2023
© The Author(s) 2023

Abstract Lipids may serve as energy reserves to support coral calcification, allow acclimation to higher temperatures, and are implicated in the control of CaCO₃ precipitation. Here, we report the lipid composition of the soft tissues (including host and symbionts) of 7 massive *Porites* spp. coral colonies (4 × *P. lutea* and 3 × *P. murrayensis*), which were cultured under different pCO₂ concentrations (180, 260, 400 and 750 µatm) and at two temperatures (25 °C and 28 °C), below the thermal stress threshold. We report the fatty acid methyl esters (FAME), free fatty acid (FFA) to total fatty acid content, sterol and wax ester profiles, and identify two ketones (*n*-alkanone) and three long chain aldehyde (*n*-alkanal) derivatives. Increasing seawater temperature significantly increases the contributions of FFAs to the total lipids, of C18:2 and C20:0 to the total FFA pool, of C14:0 to total FAME, and of campesterol to total sterol. The temperature increase also reduces the contributions of

unusual fatty acid derivatives to total lipids, of C14:0, C15:0, C16:0 and C17:0 saturated free fatty acids to total FFAs, and of C16:0 FA to total FAME. Fatty acids are implicated in the control of membrane structure fluidity and the observed changes may promote acclimation and thermostability as temperature varies. Seawater pCO₂ has no significant effect on the composition of tissue lipids with the exception that the contribution of C14:0 FA to total lipid content is significantly lower at 180 µatm compared to 260 and 750 µatm. Decreased contribution of total sterols and unusual fatty acid derivatives and increased contribution of total FFAs to total lipids are observed in the fastest calcifying coral (*a P. lutea* specimen) compared to the other corals, under all pCO₂ and temperature conditions. Although a rapid calcifier this genotype has been shown previously to exhibit pronounced abnormal changes in skeletal morphology in response to decreased seawater pCO₂. Variations in tissue lipid composition between coral genotypes may influence their resilience to future climate change.

Simon A. Young and Catherine Cole have contributed equally.

Supplementary Information The online version contains supplementary material available at <https://doi.org/10.1007/s00338-023-02356-w>.

✉ Nora S. H. von Xylander
nshvx1@st-andrews.ac.uk

✉ Terry K. Smith
tksl@st-andrews.ac.uk

✉ Nicola Allison
na9@st-andrews.ac.uk

¹ School of Biology, Biomedical Sciences Research Complex, University of St Andrews, St. Andrews KY16 9ST, UK

² School of Earth and Environmental Sciences, University of St. Andrews, St. Andrews KY16 9AL, UK

³ Graduate School of the Environment, Centre for Alternative Technology, Machynlleth SY20 9AZ, UK

Keywords Coral lipids · Calcification · Seawater temperature · pCO₂ · Ocean acidification · Biomineralisation

Introduction

Lipids are a major component of the biomass of tropical zooxanthellae corals (Patton 1977) and fulfil a range of biological functions, acting as energy reserves, precursors for hormones and vitamins, signalling molecules and membrane components (Harland et al. 1993; Imbs et al. 2010; Yamashiro et al. 1999). The neutral lipids, predominantly the triacylglycerols (TAG) and wax esters, serve primarily as energetic reserves of fatty acids, but can also be incorporated

into phospholipids and ultimately into the lipid bilayer of cell membranes (Athenstaedt and Daum 2006). Sterols are essential lipid biomolecules involved in regulating numerous cellular biological processes, including their role in sustaining biophysical properties such as cell membrane fluidity (Beck et al. 2007).

Lipids are also implicated in the control of biomineralisation (Reggi et al. 2016), the biologically controlled process by which scleractinian corals build their skeletons (Falini et al. 2015). The lipid composition of skeletal organic materials is dominated by phospholipids and sterols with waxes and sterol esters present in small amounts (Farre et al. 2010). Free fatty acids and triglycerides have also been resolved in lipid-rich skeletal samples (Farre et al. 2010). Lipids extracted from coral skeletons affect the precipitation rate, crystal morphology and porosity of CaCO₃ precipitated in vitro (Reggi et al. 2016). However, their exact role in biomineralisation has yet to be elucidated (Falini et al. 2015). Corals may catabolise lipid reserves to meet metabolic demands when growth conditions are sub-optimal (Glynn et al. 1985; Spencer Davies 1991; Grottoli and Rodrigues 2011) and tissue lipid content is used as a proxy for coral physiological condition (Anthony 2006). Field studies indicate that seasonally low coral calcification rates often coincide with periods of low coral tissue lipid biomass (Oku et al. 2003; Mehdinia et al. 2015). Interpreting this correlation is difficult as other seasonal factors may also affect coral calcification and/or lipid biomass, e.g. water temperature (Oku et al. 2003; Clausen and Roth 1975), light availability (Marubini et al. 2001), water turbidity (Carricart-Ganivet and Merino 2001), spawning (Mehdinia et al. 2015) and nutritional strategy (Seemann et al. 2012; Crandall et al. 2016).

Mixed results have been reported in the response of corals to environmental changes (Hoegh-Guldberg, et al. 2007; Fabricius et al. 2011; Pandolfi et al. 2011; Schoepf et al. 2013; Tambutté et al. 2015), where coral skeletal growth and densification were predicted to be quite sensitive to ocean acidification (Burton and Walter 1987; Doney et al. 2009). To date it appears that lipids may be involved in the response of corals to environmental changes, such as ocean acidification and rising seawater temperatures (Treignier et al. 2008; Falini et al. 2015; Grottoli et al. 2017; Coronado et al. 2019). Rapid acclimation of *Porites divaricata* to elevated seawater temperatures was observed to occur within corals having high-energy reserves and the ability to change their dominant symbiont (Grottoli et al. 2014). Other results showed a strong biological control (e.g. lipids) in the linear extension of coral skeletons (Mollica et al. 2018).

To investigate the relationship between tissue lipids, seawater temperature, and pCO₂, we analysed the tissue lipid compositions of a suite of massive *Porites* spp. corals, known to be important contributors to coral reef accretion

in the Indo-Pacific (Pichon 2011), which were maintained in laboratory aquaria at different pCO₂ and 25 or 28 °C. The 7 coral genotypes studied here exhibited widely varying calcification rates even when cultured under similar conditions (Cole et al. 2018) and we explore the relationships between calcification rate, lipid compositions and seawater temperature/pCO₂. We utilised modern sensitive mass spectrometric approaches to probe more detailed information about the lipid composition of each individual.

Methods

Coral culturing

We cultured massive *Porites* spp. corals over a range of seawater pCO₂ (180, 260, 400 and 750 µatm) and at either 25 or 28 °C in two experiments, previously described (Cole et al. 2016, 2018). These pCO₂ reflect conditions in the Last Glacial Maximum, the preindustrial, the present day and a potential future pCO₂ scenario (Barry et al. 2011). Both temperatures are within the seasonal range observed at the coral collection site (Fiji) and are assumed to be below the thermal stress threshold.

Large coral heads were imported and maintained in a purpose-built aquarium system at the University of St Andrews, U.K. For each experiment, we sawed the heads into multiple pieces (sub-colonies, each ~ 12 cm in diameter) so that at least one large sub-colony could be cultured in each seawater pCO₂ treatment. The coral heads were considered to represent different genotypes when they were collected from spatially separate (non-adjointing) colonies. We used large sub-colonies (each > 12 cm diameter) in each treatment, as small experimental colonies are not indicative of the physiological performance of larger colonies (Edmunds and Burgess 2016).

Coral sub-colonies were housed in 21 L cast acrylic tanks supplied with seawater from large (900 L) high-density polyethylene seawater reservoirs bubbled with air at the required CO₂ composition at 10L min⁻¹ (Cole et al. 2018). A 12 h light: 12 h dark cycle was programmed with LED lighting (Maxspect R420R 160w-10000 k), and wavelength settings of 100% A and 20% B, such that light intensity at coral depth was approximately 300 µmol photons m⁻² s⁻¹. Corals were fed weekly with rotifers, and samples for lipid analyses were collected > 72 h after feeding. Zooplankton digestion in corals takes 1–3 days (Leal et al. 2014) and we consider that undigested rotifers do not contribute to the total coral lipids.

The total alkalinity, [Ca] and [Sr] of the culture seawater were maintained within narrow limits (Cole et al. 2016, 2018) by automated 200 µL additions of 0.6 M Na₂CO₃ and 0.58 M CaCl₂ + 0.02 M SrCl₂ evenly spaced

over a 24 h period. Automated variable speed powerheads (VorTech, Ecotech Marine, USA) in the coral tanks created a chaotic water flow mimicking that of a high-energy reef environment.

In the first experiment, corals were maintained at target pCO₂ and 25 °C for > 6 months before sampling. In the second experiment, the same sub-colonies were maintained at target pCO₂ throughout but at 2 temperatures at different times of the experiment. Corals were initially kept at 28 °C for > 5 months before parts of the sub-colonies (~25% of total) were removed by saw for lipid analysis. The temperature was then decreased to 25 °C over a period of 1 month, while the sawn colony edges were overgrown with fresh coral tissue. Sub-colonies were held at 25 °C for at least 2 more months before lipid sampling.

Tissue sampling and lipid extraction

We analysed the lipids in tissues from 7 coral genotypes from both experiments (3 from experiment 1 and 4 from experiment 2), and we adopt the same genotype numbering convention used in Cole et al. (2018). Corals were identified to species level using the skeletal corallite structure (Veron 2000). Three colonies were identified as *P. murrayensis* and four colonies as *P. lutea*, although we note that molecular markers indicate that globally, corals identified as this species fall into three genetically distinct groups (Forsman et al. 2009).

To obtain samples, small blocks (~2 × 2 cm), including skeleton and overlying tissue, were sawn from the central area of each sub-colony and flash-frozen in liquid nitrogen. Replicate samples were taken from 5 sub-colonies to test for variability in tissue lipids. After thawing, the coral tissue was blasted from the skeleton with fresh artificial seawater using an artist's airbrush and collected in 15-mL plastic centrifuge tubes on ice. This method may result in incomplete removal of the tissue from the skeleton (Conlan et al. 2017) resulting in underestimation of both tissue and lipid biomass. However, the alternative (crushing the tissue and skeleton in the lipid extractant) results in the contamination of the tissue lipids by skeletal lipids which are present in the coral aragonite in different compositions to the coral tissue (Farre et al. 2010) and in endolithic algae and fungi (Le Campion-Alsumard et al. 1995a, b). The chosen technique resulted in the tissue lipid extraction of the whole coral holobiont, thus including any tissue lipids that might be present in the coral host, algal symbiont, and microbiome present (Goulet et al. 2020).

The tissue-seawater slurry was centrifuged (3000 rpm, 4 °C, 15 min), the supernatant seawater was removed, and the pelleted tissue was frozen at -20 °C, freeze-dried, and weighed to give a dry tissue weight. The dry tissue was homogenised by vortex in 1 mL PBS and then transferred

to a pre-weighed glass vial. The lipid fraction was extracted following the method of Bligh and Dyer (1959): A mixture of chloroform and methanol (1:2 v/v) was added to the homogenised tissue, vortexed, and agitated on a shaking platform at 4 °C overnight. Samples were then brought to room temperature, and the lipid phase was separated by successive additions of chloroform and deionised water. The biphasic samples were centrifuged at room temperature (800 × g, 10 min), and the lower lipid phase was carefully withdrawn with a pipette. Finally, the total lipid extract was dried under a stream of nitrogen and weighed.

We analysed the free fatty acid (FFA), sterol, wax esters, and fatty acid methyl ester (FAME) compositions of all of the coral samples and performed high-performance thin layer chromatography (HPTLC) on a subset of the samples.

HPTLC

Lipid extracts were separated by high-performance thin layer chromatography (HPTLC) for a subset of G1 (*P. lutea*), G3 (*P. murrayensis*), and G5 (*P. lutea*) sub-colonies cultured at 25 °C. Dried lipid samples were re-suspended in a volume of chloroform/methanol (2:1 v/v) such that an 8 µL aliquot contained 50 µg of lipid. Samples of 50 µg lipid were applied to 10 cm × 10 cm HPTLC plates (Merck), and the plates were developed to full height in equilibrated tanks containing, successively, hexane and then toluene. Finally, plates were developed to half height in hexane:ether:acetic acid (70:30:1, v/v/v). After air-drying, plates were developed using a fine spray of phosphoric acid/33% acetic acid/sulfuric acid/0.5% copper sulphate (5:5:0.5:90, by vol.) and heated at 100 °C for 15 min. The plates were scanned under UV light, and Image Quant TL software was used to measure spot intensity of the separated lipid fractions. Relative abundance of each lipid class was estimated as a % of the total lipid. A synthetic mix containing a sterol ester (cholesterol palmitate), TAG (tristearin), free fatty acid (C18:1), and sterol (cholesterol) was used as a standard alongside the samples to confirm the identity of the spots.

Analysis of free fatty acids, sterols, and wax esters

An appropriate amount of lipid extract was dissolved in 20 µL dichloromethane, and 1 µL was analysed by gas chromatography-mass spectrometry (GC-MS). An Agilent Technologies mass selective detector (GC-6890N, MS detector-5973) was used, with a ZB-50 column (15 M × 32 mm ID × 0.5 mm thickness, (Phenomenex)), injector at 270 °C with a temperature programme of 100 °C for 1 min followed by a rising gradient to 200 °C at 8 °C/min and held at 200 °C for a further 2 min, followed by a second gradient at 3 °C/min up to 300 °C for a further 15 min. Mass spectra were acquired from 50 to 550 amu, and sterol and other lipids

were identified by comparison with a range of standards purchased from Sigma and Matreya. The relative proportions of individual molecular species within each lipid class were calculated as a % of the total within that class.

FAME analysis

The global fatty acid composition of coral lipids was analysed by the conversion to FAME. Total fatty acids were isolated from the *Porites* lipid extracts and converted to FAME for GC–MS characterization following the method of Ichihara and Fukubayashi (2010). This trans-methylation reaction forms methyl esters of all fatty acids in the sample, regardless of the lipid they were attached to. Lipid samples were suspended in 300 μL of 8% (w/v) solution of HCl in methanol water (85:15 v/v) and 200 μL of toluene and 1.5 mL of methanol were added prior to incubation overnight at 45 °C. Samples were dried down under nitrogen and 500 μL hexane and 500 μL distilled water were added to create a biphasic mixture, of which the FAME containing upper hexane layer was extracted and dried again under nitrogen. FAME samples were dissolved in 20 μL dichloromethane and analysed by injection of 1 μL into an Agilent Technologies GC–MS (GC-6890N, MS detector-5973) using a ZB-5 column (30 M \times 25 mm \times 25 mm, Phenomenex) with a temperature programme of 50 °C for 10 min followed by a rising gradient to 220 °C, at 5 °C /min and held at 220 °C for a further 15 min. Mass spectra were continuously acquired in the range of 50–500 amu, and peak identification was performed by comparison of the retention times and fragmentation patterns with a bacterial FAME standard mixture that contains both odd and even fatty acid chains (SIGMA Supelco 47,080-U).

Statistical analysis

A preliminary review of the data indicated that large variations in lipid composition were observed between some coral genotypes. We focus statistical analyses on the corals from experiment 2 (G4–G7) as sub-colonies of these genotypes were cultured at each pCO₂ and temperature. Significant differences ($p \leq 0.05$) in lipid composition between pCO₂ treatments and genotypes are tested using one-way ANOVA followed by a Tukey post hoc test in R studio. Both temperatures and either all pCO₂ treatments or genotypes are combined for analysis. We test for differences in the contribution of each lipid group to total lipid class (e.g. each sterol group to total sterols) at 25 °C and 28 °C using a paired *t*-test, matching the lipid data for each individual sub-colony at 25 °C and 28 °C for each pair. A similar approach is used to compare the ratios of unsaturated to saturated fatty acids and fatty acid methyl esters, as well as for the ratio of

n-alkanal to n-alkalone fatty acid derivatives as a function of temperature.

Results

HPTLC

Free (non-esterified) sterols are the dominant lipid class present in both coral species, contributing 24–51% of the total spot volume (Fig. 1a). Sterol esters make up 14–21%; wax esters 8–13%; monoalkyldiacylglycerols (MADAG) 6–13%; triacylglycerols (TAG) 11–16%; and free fatty acids (FFAs) 9–14%. These relative spot intensities do not translate directly to lipid proportions in the tissue, since each lipid class consists of a range of lipid species with different masses, but they can be useful for highlighting key differences between coral lipid profiles. No significant differences were found for all the lipid classes between the different pCO₂ treatments. Phospholipids do not migrate away from the origin in this solvent system and so cannot be quantified by densitometry.

GC–MS

We observe excellent separation of the free fatty acids, sterols and wax esters in both *P. lutea* and *P. murrayensis* samples (Fig. 1b, c), enabling relative quantification of the abundance of individual lipid species within these classes.

Sterols

GC–MS analysis detected 7 different sterol species (Fig. 1b, peaks o, p, r–u, w). Variations in total sterol, stigmasterol, brassicasterol and fucosterol between corals are shown in Fig. 2, whilst variations in all sterols are shown as a heat map in supplementary Fig. 1. Campesterol and stigmasterol are the most abundant sterols in both genotypes, followed by brassicasterol with cholesterol, C29, C30, and fucosterol each contributing ~ 1% of the total sterol composition (Supplementary Fig. 2). We observe no significant effect of seawater pCO₂ on sterol composition (Table 1 and Supplementary table 1), but increasing temperature causes a significant increase in the contribution of campesterol to total sterol. Stigmasterol contributes a significantly higher proportion of the total sterol in genotype G7, while brassicasterol contributes a significantly higher proportion of total sterol in G5 compared to the other corals (Fig. 2b and c). Fucosterol is identified only in the G5 and G7 *P. lutea* coral colonies (Fig. 2d). Total sterols make a significantly smaller contribution to total lipids in G7 than in the other genotypes tested (Fig. 2a, Table 1 and supplementary Table 1).

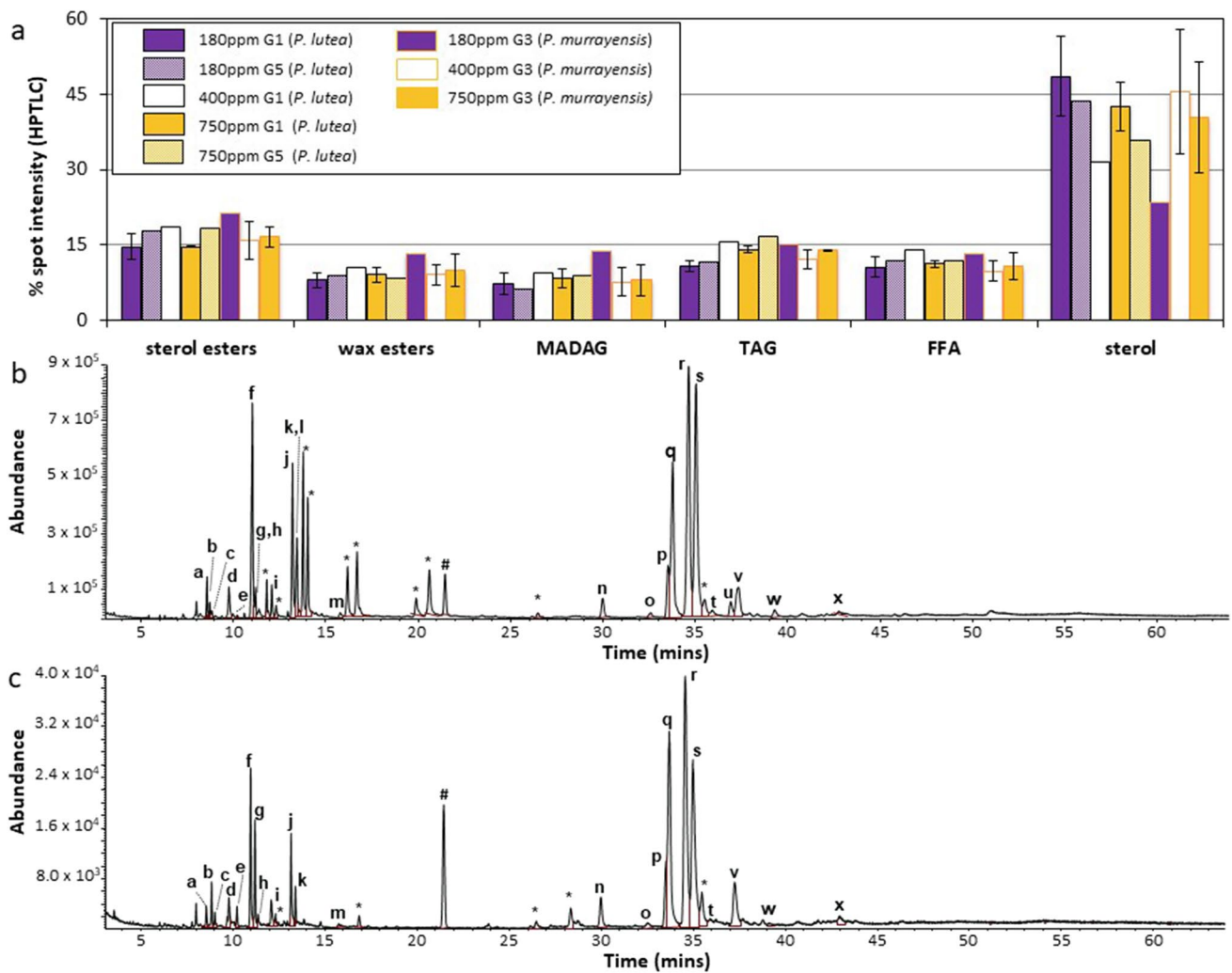


Fig. 1 Composite image of the HPTLC spot sizes and GC–MS spectra. **a** shows the spot intensity for each of the lipid classes (sterol ester, wax ester, monoalkyldiacylglycerol (MADAG), triacylglycerol (TAG), free fatty acid (FFA), and sterol) as a % of the total spot intensity, in coral tissue extracts separated by HPTLC. Error bars show $\pm 1\sigma$ of the mean from duplicate samples. **b** and **c** show repre-

sentative spectra of the total ion current chromatogram of the total lipid extracts from *P. lutea* and *P. murrayensis* samples, respectively. Lettering denotes free fatty acids (a, d, f, i–m), *n*-alkanones (b, g), *n*-alkanals (c, e, h), wax esters (n, q, v, x) and sterols (o, p, r–u, w). Unidentified putative apocarotenoids are indicated by * while # shows a common GC–MS contaminant dibutylphthalate (plasticiser)

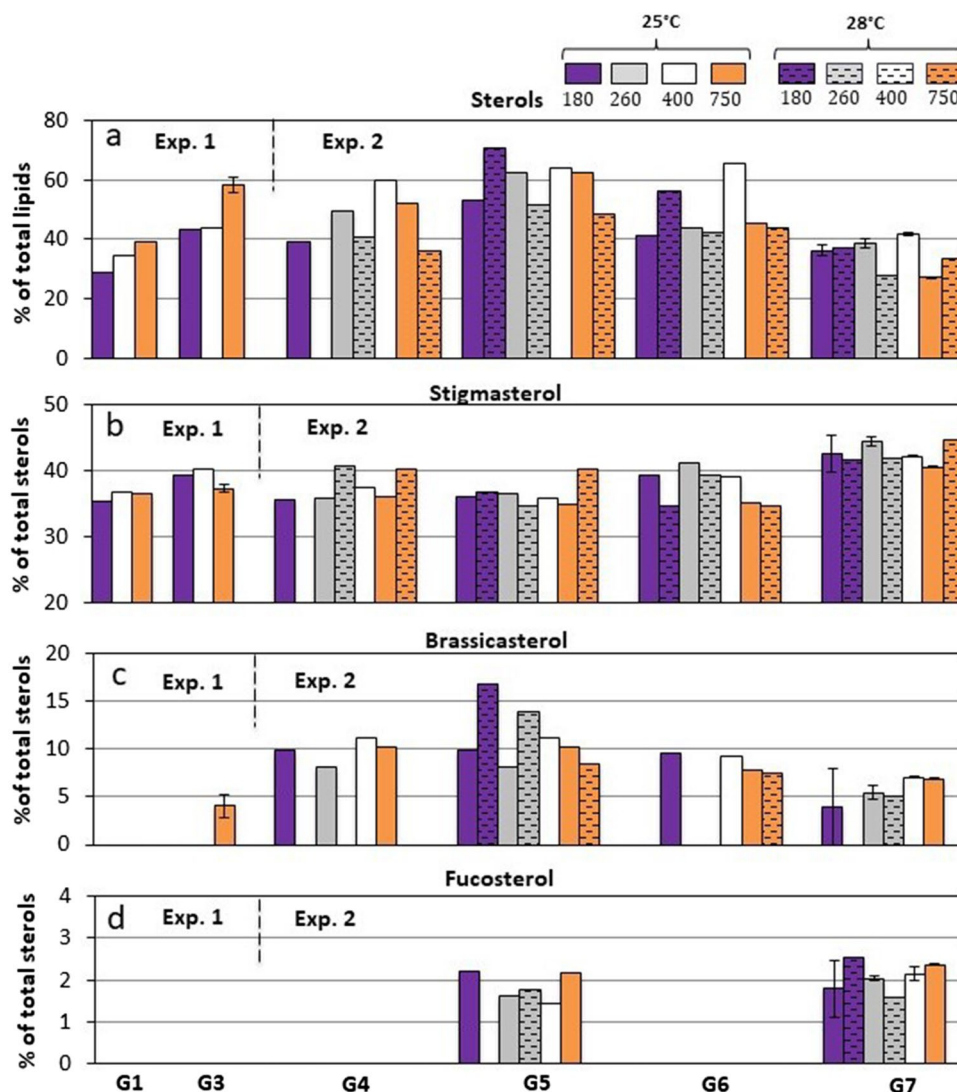
Wax esters

Four different wax esters were identified (Fig. 1b, c, peaks n, q, v, x) of which C32 palmityl-palmitate was dominant (typically > 70% of total wax esters, Supplementary Fig. 3). The remaining wax esters are largely composed of two isomeric mixtures: C34 palmityl stearate/stearyl palmitate and C30 myristyl palmitate/palmityl myristate, whilst a larger (C36 linoleyl stearate) wax ester is present at ~1%. No significant differences are observed in the contributions of each wax esters to the total between pCO₂ treatments or coral genotype. (Table 1; supplementary Fig. 4 and supplementary Table 2).

Free fatty acids

GC–MS analysis identifies a mixture of saturated and unsaturated free fatty acids (FFAs) (Fig. 1b, c, peaks a, d, f, i–m). Variations in all FFAs are shown as a heat map in Fig. 3, with their relative compositions shown in supplementary Fig. 5. Variations in total FFAs, myristic acid, palmitic acid, linoleic acid, and linolenic acid, across the different pCO₂ and temperature treatments are shown in supplementary Fig. 6. Palmitic acid (C16:0) and stearic acid (C18:0) are the most abundant FFAs in all coral genotypes. Odd chain fatty acids C15:0 and C17:0 and polyunsaturated fatty acids (PUFAs): C18:2 and C18:3 typically contribute 5–10% each to FFAs. No significant differences are observed in the

Fig. 2 Bar graphs showing the contribution of **a** sterols to total lipids, as well as **b** stigmasterol **c** brassicasterol **d** fucosterol to the total sterols identified through GC–MS analysis. G4 to G7 *Porites* genotypes were cultured during experiment 2 at different pCO₂ (180, 260, 400, 750 ppm) and either 25 °C or 28 °C, whilst G1 and G3 were cultured during experiment 1 at 400 ppm & 25 °C. Error bars show $\pm 1\sigma$ of the mean from duplicate samples



contributions of each FFA to the total between CO₂ treatments, but increasing temperature significantly increases the contributions of the polyunsaturated FFA C18:2, as well as C20:0, whilst decreasing the contributions of saturated FFAs C14:0, C15:0, C16:0, and C17:0 (Table 1 and Supplementary table 3). Total FFAs were significantly higher at 28 °C compared to 25 °C. In the G7 colony myristic acid (C14:0), C17:0, and linoleic acid (C18:2) make a significantly smaller contribution to the total FFAs than in the other experiment 2 genotypes, while linolenic acid (C18:3) makes a greater contribution. An overall higher contribution of total FFAs is found within the G7 colony. Some other minor differences in FFA composition are observed between the other corals.

Unusual FA derivatives and other lipids

We observe for the first time in *Porites* spp. corals the presence of unusual fatty acid derivatives (Fig. 1b, c). Two

n-alkenones: C16 (hexadecan-2-one) and C18 (octadecan-2-one) (Fig. 1b, c, peaks b and g) and three *n*-alkanals C16 (hexadecanal), C17 (heptadecanal) and C18 (octadecanal) (Fig. 1 peaks c, e and h) have been identified. Variations in the total unusual fatty acid derivatives, as well as hexadecan-2-one, and octadecanal between corals and varying conditions are shown in Fig. 4, whilst variations in all detected unusual fatty acid derivatives can be found as a heat map in supplementary Fig. 8. Octadecan-2-one, octadecanal, and hexadecan-2-one are the most abundant unusual FA derivative detected (supplementary Fig. 7). The relative total abundance of the *n*-alkanals is noticeably lower than the *n*-alkenones in all genotypes except for the G1 *P. lutea* genotype. We observe no significant effect of seawater pCO₂ on FA derivatives, but the contribution of FA derivatives to total lipids is significantly lower at the high seawater temperature and within the G7 coral colony (Fig. 4a, Table 1, and Supplementary table 4). Octadecanal makes a significantly

Table 1 Summary table of statistical results obtained from pooling together all corals cultured under experiment 2. All corals of all genotypes were pooled together to test for differences between pCO₂ treatments, whilst all corals of the same genotype regardless of pCO₂ were pooled together to test for differences between genotypes by one-way ANOVA analysis using R studio. Paired *t* tests were used to compare the lipid compositions of samples cultured at 25 °C and 28 °C. Any non-significant differences found during analysis are denoted as n.s. in the table

	Temperature	pCO ₂	Genotype
Stigmasterol	n.s	n.s	G7 > G4, G5, G6
Campesterol	25 < 28	n.s	G5 < G4, G6, G7
Brassicasterol	n.s	n.s	G5 > G6, G7
Fucosterol	n.s	n.s	G5, G7 > G4, G6
C29 sterol	n.s	n.s	G6 > G5, G7
Total sterols	n.s	n.s	G7 < G5, G6
Myristyl palmitate (C30)	25 > 28	n.s.	n.s
Palmityl palmitate (C32)	n.s	n.s	n.s
Stearyl palmitate (C34)	n.s	n.s	n.s
Total wax esters	n.s	n.s	n.s
Myristic acid (C14:0)	25 > 28	n.s	G7 < G5, G6
Pentadecanoic acid (C15:0)	25 > 28	n.s	n.s
Palmitic acid (C16:0)	25 > 28	n.s	G6 > G5, G7
Heptadecanoic acid (C17:0)	25 > 28	n.s	G7 < G4, G5, G6
Stearic acid (C18:0)	n.s	n.s	n.s
Linoleic acid (C18:2)	25 < 28	n.s	G7 < G4, G5, G6
Linolenic acid (C18:3)	n.s	n.s	G7 > G4, G5, G6
C20:0	25 < 28	n.s	G6 < G5
Total free fatty acids	25 < 28	n.s	G7 > G4, G5, G6
Hexadecan-2-one (C16)	n.s	n.s	G7 < G6
Octadecan-2-one (C18)	n.s	n.s	n.s
Octadecanal (C18)	n.s	n.s	G7 > G6
Total fatty acid derivatives	25 > 28	n.s	G7 < G4, G6
Fatty acid methyl ester C14:0	25 < 28	180 < 260, 750	n.s
Fatty acid methyl ester C15:0	25 > 28	n.s	n.s
Fatty acid methyl ester C16:0	25 > 28	n.s	G5 < G4, G6, G7
Fatty acid methyl ester C17:0	n.s	n.s	G5 > G7
Fatty acid methyl ester C18:0	n.s	n.s	G7 > G4, G6
Fatty acid methyl ester C18:1	n.s	n.s	n.s
Fatty acid methyl Ester C18:2	n.s	n.s	n.s
Fatty acid methyl ester C20:0	n.s	n.s	G5 > G4, G6, G7
Unsaturated:saturated FFAs	n.s	n.s	n.s n.s
Unsaturated:saturated FAME n-alkanal:	n.s	n.s	n.s
<i>n</i> -alkanone FAdS	n.s	n.s	n.s

higher contribution to total FA derivatives in G7, while hexadecan-2-one makes a significantly lower contribution. In addition, there are a number of putative apocarotenoids present in variable amounts in the genotypes, though the specific identification of each pigment remains unknown at this time.

FAME analysis

The total fatty acid content of the tissue is determined utilising fatty acid methyl esters (FAME) analysis, which identifies a mixture of saturated and unsaturated fatty acids (FAs), similar to the detected FFAs through GC–MS analysis. Variations in the subset of FAMES identified in this study are shown as a heat map in Fig. 5, with their relative

compositions shown in supplementary Fig. 9. Variations in C14:0, C16:0, C17:0, C18:0, and C20:0 FAME, across the different pCO₂ and temperature treatments, are shown in supplementary Fig. 10. C16:0 is the most abundant FAME (58 ± 2%), and C18:0 is also a significant contributor within all coral genotypes (24 ± 2%). Unsaturated fatty acids C18:1 and C18:2 make a minor contribution total FAME in both *P. lutea*, and *P. murrayensis*. Increasing seawater pCO₂ increases the contribution of C14:0 to total FAME but otherwise has no other significant effects (Table 1 and supplementary table 5). Increasing seawater temperature increases the contribution of C14:0 and decreases the contributions of C15:0 and C16:0. A significantly lower portion of C16:0 to total FAME, and a significantly higher portion of C17:0 and C20:0 to total

		% of total FFAs							% total lipids Total FFAs	
		C14:0	C15:0	C16:0	C17:0	C18:0	C18:2	C18:3		C20:0
Experiment 1	G1 180ppm 25°C	7.0	7.4	43	5.6	27	5.6	0.0	4.6	19
	G1 400ppm 25°C	4.5	9.0	42	7.6	26	5.5	0.0	5.5	16
	G1 750ppm 25°C	7.1	3.7	37	3.9	25	14	3.5	5.3	23
	G3 180ppm 25°C	6.1	3.4	34	5.7	25	22	3.6	0.0	18
	G3 400ppm 25°C	5.3	8.4	39	11.4	23	8	0.0	4.6	13
	G3 750ppm 25°C	6.4	5.1	37	8.5	21	15	3.1	4.3	17
	G4 180ppm 25°C	6.8	6.0	33	6.3	24	20	2.2	2.4	14
	G4 260ppm 25°C	6.7	3.6	34	5.5	20	26	4.8	0.0	20
	G4 260ppm 28°C	6.6	3.4	26	5.1	16	33	4.3	5.9	21
	G4 400ppm 25°C	5.5	4.4	40	6.7	31	12	0.0	0.0	15
	G4 750ppm 25°C	9.4	5.9	34	7.4	20	19	3.7	0.0	16
	G4 750ppm 28°C	6.8	3.5	25	4.0	18	27	4.5	10.1	24
	G5 180ppm 25°C	7.4	5.5	35	6.5	22	20	0.0	4.5	16
	G5 180ppm 28°C	5.0	3.0	27	4.3	18	19	5.3	17.7	17
Experiment 2	G5 260ppm 25°C	9.0	5.8	29	4.5	18	23	2.8	7.9	18
	G5 260ppm 28°C	6.1	3.6	27	5.0	21	20	2.3	15.4	18
	G5 400ppm 25°C	9.9	5.9	38	7.1	21	18	0.0	0.0	13
	G5 750ppm 25°C	7.5	3.4	27	5.3	16	26	3.4	11.1	15
	G5 750ppm 28°C	6.9	2.6	24	3.9	19	22	3.6	17.8	20
	G6 180ppm 25°C	9.4	7.6	37	7.9	21	17	0.0	0.0	15
	G6 180ppm 28°C	6.6	3.7	33	6.1	18	29	3.9	0.0	20
	G6 260ppm 25°C	7.0	6.9	39	7.5	22	18	0.0	0.0	14
	G6 260ppm 28°C	7.4	4.3	30	6.4	16	26	3.3	7.0	20
	G6 400ppm 25°C	7.0	4.4	38	6.8	21	23	0.0	0.0	12
	G6 750ppm 25°C	10.3	7.3	41	6.3	22	14	0.0	0.0	20
	G6 750ppm 28°C	7.4	4.2	31	5.5	21	17	2.7	10.8	19
	G7 180ppm 25°C	4.4	5.5	27	3.7	25	13	12.9	8.8	26
	G7 180ppm 28°C	3.8	3.9	26	3.6	20	17	13.7	12.7	27
G7 260ppm 25°C	5.8	5.0	33	3.4	22	13	11.7	5.5	30	
G7 260ppm 28°C	5.5	5.0	26	3.3	26	15	10.0	9.3	27	
G7 400ppm 25°C	3.8	4.8	30	3.9	19	12	18.6	8.5	26	
G7 750ppm 25°C	8.6	4.6	27	3.2	27	14	9.1	5.6	29	
G7 750ppm 28°C	5.5	4.8	29	3.4	26	12	6.3	13.2	34	

Fig. 3 Heat map showing the relative composition of free fatty acids (FFAs) measured by GC–MS in 6 of the *Porites* spp. colonies cultured under varying pCO₂ and temperature. Relative concentrations are presented as percentages of the total of all FFAs, as well as a total

of all FFAs to total lipids. G1 & G3 genotypes were cultured under experiment 1 at either 180, 400, or 750 ppm and 25 °C, whilst experiment 2 genotypes (G4, G5, G6 & G7) were cultured under varying pCO₂ (180, 260, 400, & 750 ppm) and at either 25 °C or 28 °C

FAME are detected within the G5 coral colony in Experiment 2. C18:0 FAME is significantly higher within the G7 *P. lutea* genotype compared to G4 and G6 *P. murrayensis* genotypes within experiment 2.

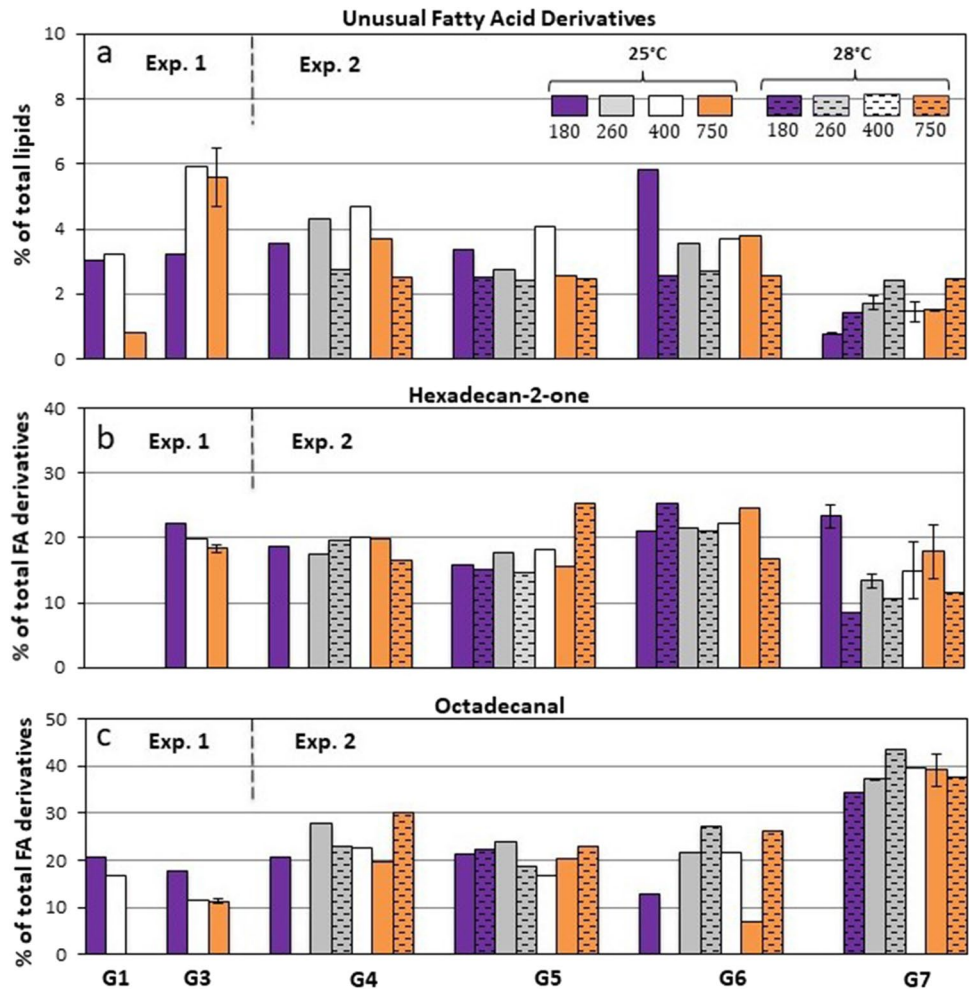
Ratios of unsaturated versus saturated lipid classes

Here, we report the ratios of total unsaturated versus total saturated, free fatty acids, fatty acid methyl esters, or the ratios comparing *n*-alkanal fatty acid derivatives to *n*-alkalone (Fig. 6). No significant differences are found, when comparing between either temperatures, pCO₂ treatments, or genotypes, (Table 1 and supplementary table 6).

Lipid concentration and calcification rate

The calcification rates of each coral sub-colony were measured 2–4 times in the 4 weeks period preceding tissue sampling using the alkalinity anomaly technique under both light and dark conditions (Cole et al. 2018). Here, we plot calcification rate as a function of the different percentage contribution of lipid classes to total lipids detected through GC–MS analysis (Fig. 7). We observe significant negative relationships between % contribution of both sterols and unusual FA derivatives to total lipids versus coral calcification rate. We also observe significant positive relationships between the % contribution of both FFAs and wax esters to total lipids versus coral calcification rate. Genotype G7 had a higher calcification rate at all pCO₂ and temperatures compared to the other corals, and if we remove this genotype from the data set, then the relationships between calcification rate and the

Fig. 4 Bar graphs showing the contribution of **a** unusual fatty acid derivatives to total lipids, as well as **b** hexadecan-2-one, and **c** octadecanal, to the total unusual fatty acid derivatives identified through GC–MS analysis, for the 4 different *Porites* spp. genotypes cultured during experiment 2 at increasing pCO₂ (180, 260, 400, 750 ppm) and either 25 °C or 28 °C. Experiment 1 G1 and G3 genotypes are also added to allow comparison between experiments. Error bars show $\pm 1\sigma$ of the mean from duplicate samples



% contributions of both FFAs and unusual FA derivatives to total lipids become insignificant.

Discussion

Lipids in the coral holobiont are derived from algal biosynthesis (Muscatine 1990; Papina et al. 2003; Teece et al. 2011; Baumann et al. 2014), coral biosynthesis (Chen et al. 2021), heterotrophic feeding (Tolosa et al. 2011), and conversions between existing lipids in the holobiont. The tissue sterol compositions in the present study are dominated by campesterol, stigmasterol, and brassicasterol (supplementary Fig. 2), which are all phytosterols previously observed in marine algae

(Abdul et al. 2016; Lee et al. 2020). Heterotrophic feeding enhances the abundance of unsaturated fatty acids in coral tissues (Imbs 2013), and the low abundance of these forms in our samples (supplementary Fig. 5 and 9) likely indicates that the corals were predominantly autotrophic. The observed odd-chain fatty acids and unusual fatty acid derivatives may originate from endosymbiotic bacteria within the coral host (Kaneda 1991; Al-Lihaibi 2007; Tolosa et al. 2011).

		% of total FAME							
		C14:0	C15:0	C16:0	C17:0	C18:0	C18:1	C18:2	C20:0
Experiment 1	G1 180ppm 25°C	4.6	1.4	58	2.6	22	5.1	4.5	1.0
	G1 400ppm 25°C	1.9	1.3	58	2.6	27	3.1	4.5	1.4
	G1 750ppm 25°C	7.9	0.0	69	0.0	19	0.0	4.1	0.0
	G3 180ppm 25°C	7.1	1.2	57	2.0	20	6.2	4.0	2.2
	G3 400ppm 25°C	4.2	2.0	56	4.3	25	4.8	2.5	1.1
	G3 750ppm 25°C	7.6	1.8	57	3.9	24	1.4	2.4	1.3
	G4 180ppm 25°C	6.5	1.7	63	1.8	18	0.0	7.0	2.7
	G4 260ppm 25°C	7.9	0.0	62	1.8	22	0.4	5.0	0.6
	G4 260ppm 28°C	12.1	0.7	58	1.5	17	1.7	5.1	4.2
	G4 400ppm 25°C	8.5	1.8	57	2.8	24	0.0	4.4	0.9
Experiment 2	G4 750ppm 25°C	8.5	1.5	58	2.8	19	4.3	5.2	0.6
	G4 750ppm 28°C	13.2	0.5	58	2.3	19	2.2	4.8	0.8
	G5 180ppm 25°C	6.9	2.0	53	2.5	21	5.5	5.1	3.7
	G5 180ppm 28°C	8.4	1.4	47	4.3	24	5.5	5.2	4.6
	G5 260ppm 25°C	13.2	1.4	52	2.6	19	3.5	4.8	2.8
	G5 260ppm 28°C	9.7	0.0	54	3.6	20	5.3	5.2	1.5
	G5 400ppm 25°C	7.8	1.8	58	3.5	23	0.0	3.4	2.2
	G5 750ppm 25°C	8.6	1.7	53	3.9	24	1.9	4.2	3.2
	G5 750ppm 28°C	10.3	1.1	50	4.3	22	3.5	5.5	3.2
	G6 180ppm 25°C	7.7	2.4	59	2.8	21	0.8	4.3	2.0
	G6 180ppm 28°C	9.7	1.7	57	2.5	19	4.1	4.2	1.1
	G6 260ppm 25°C	8.8	1.4	53	2.3	18	8.1	7.3	2.0
	G6 260ppm 28°C	10.6	1.4	56	3.5	19	2.5	4.7	2.9
	G6 400ppm 25°C	8.3	2.1	57	2.5	23	2.0	4.1	1.9
	G6 750ppm 25°C	9.9	2.3	63	0.0	19	2.4	3.0	0.0
	G6 750ppm 28°C	12.0	0.0	62	1.5	19	0.0	4.5	0.9
	G7 180ppm 25°C	4.9	1.2	61	2.2	24	0.3	4.3	1.6
G7 180ppm 28°C	6.4	1.1	58	4.2	22	3.5	4.1	0.7	
G7 260ppm 25°C	8.0	1.5	60	2.4	21	0.6	3.8	2.3	
G7 260ppm 28°C	9.5	1.0	55	1.6	24	2.7	4.9	1.3	
G7 400ppm 25°C	5.7	1.2	62	1.6	23	0.4	4.4	1.7	
G7 750ppm 25°C	10.8	0.4	58	1.1	21	2.0	4.8	1.6	
G7 750ppm 28°C	7.9	0.0	57	1.9	27	3.1	3.1	0.0	

Fig. 5 Heat map showing the relative composition of fatty acid methyl esters (FAME) measured by GC–MS in 6 of the *Porites* spp. colonies cultured under varying pCO₂ and temperatures. Relative concentrations are presented as percentages of the total of all FAME. Experiment 1 G1 & G3 genotypes were cultured at either 180, 400,

or 750 ppm and 25 °C, whilst experiment 2 genotypes (G4, G5, G6 & G7) were cultured under varying pCO₂ (180, 260, 400, & 750 ppm) and at either 25 °C or 28 °C. Error bars show $\pm 1\sigma$ of the mean from duplicate samples

The influence of environmental change on coral tissue lipids

Temperature

Raising temperature (from 25–28 °C) increases the contribution of FFAs to total lipid and the contribution of unsaturated FFA C18:2 to the total FFA pool, but decreases the contribution of the saturated FFAs C14:0, C15:0, C16:0 & C17:0 to total FFAs and of C16:0 to the total fatty acid (FAME) of the total lipids, as well as the total contribution of unusual FA derivatives to total lipids (Table 1). Fatty acids (FA) represent a large group of molecules that are utilised by the majority of lipid classes found within organisms, playing a wide range of roles in mechanisms, such as cell

signalling, membrane structure fluidity, and energy storage (Samori et al. 2017). The compositions of both the FFAs and the fatty acid components of all lipids (FAME) in this study are dominated by C16:0 and C18:0, with C18:3 (an omega-3 fatty acid) also making a significant contribution (Figs. 3, 5). These are the predominant fatty acid species previously identified in *Porites* spp. field corals (Harland et al. 1991; Latyshev et al. 1991) and C16:0 and C18:0, are the key precursors for the biosynthesis of polyunsaturated fatty acids (e.g. 18:2 and 18:3) (Al-Moghrabi et al. 1995), and are essential building blocks for a range of other lipid species (Imbs 2013). A twofold increase in FFAs occurred in *Acropora intermedia* under acute heat stress (Imbs & Yakovleva 2012), but the changes in this study (when the

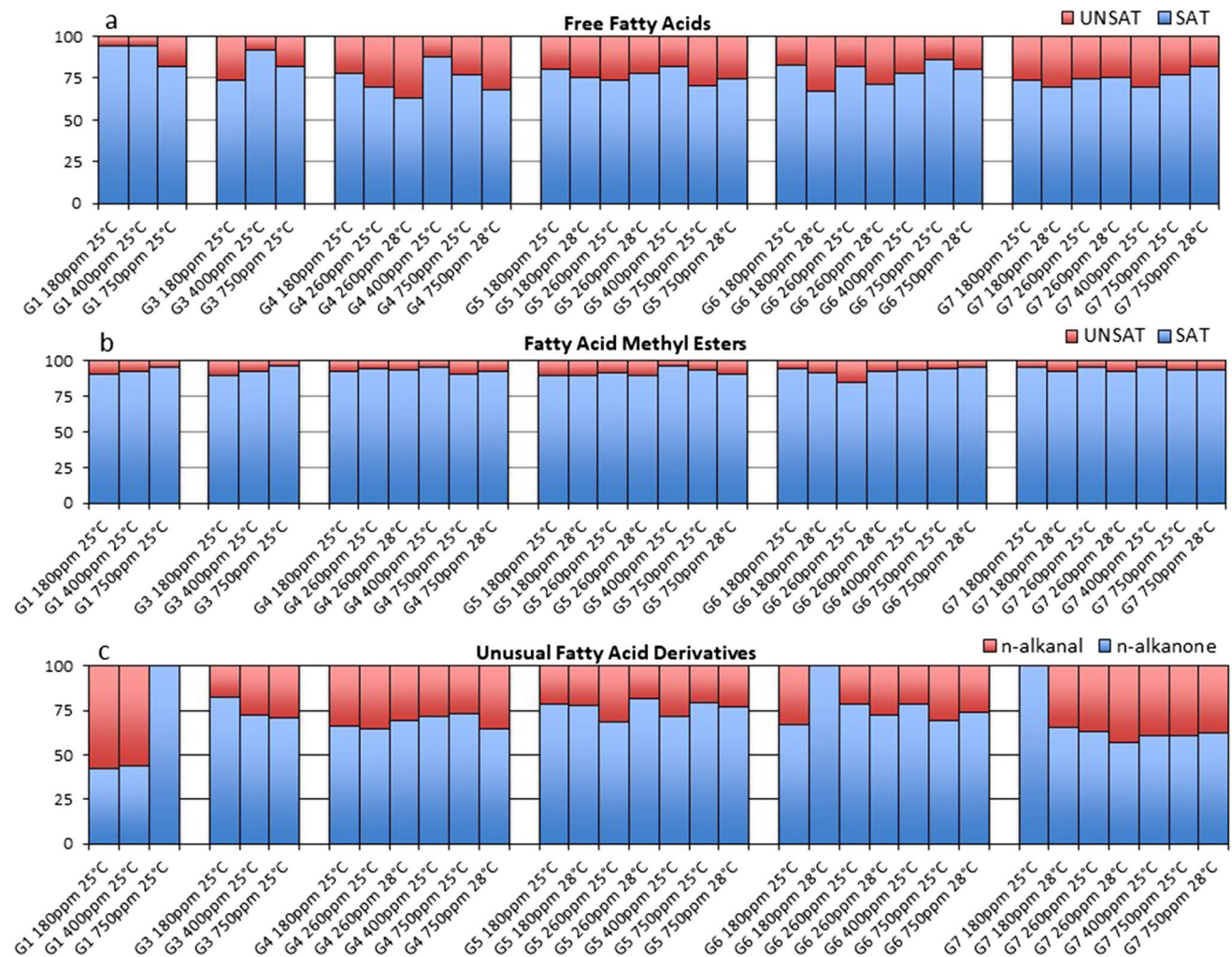


Fig. 6 Bar graphs showing the ratios of total unsaturated (UNSAT) versus total saturated (SAT) **a** free fatty acids **b** fatty acid methyl esters, or **c** the ratios comparing n-alkanal fatty acid derivatives to

n-alkanone, identified through GC–MS analysis, for both experiment 1 and 2 *Porites* spp. genotypes cultured at varying pCO₂ and at either 25 °C or 28 °C

thermal stress threshold of the corals was not breached) are much more subtle.

Palmitate, C16:0 is respired during periods of increased energy consumption to maintain coral metabolism (Tolosa et al. 2011) and is the dominant fatty acid in the triglycerides (TAGs) of reef building corals (Yamashiro et al. 1999; Imbs 2013). The reduced contribution of C16:0 to both FFAs and FAME at high temperature in this study could reflect catabolism of TAGs in response to increased temperature. However, a decrease in the contribution of a specific FFA to total FFA at high temperature does not necessarily imply that the tissue concentration of the specific FFA has decreased. As total FFAs increase at high temperature (by on average 3%), minor decreases in the contributions of specific FFAs, e.g. C14:0 (decreased by 2%) to total FFAs may reflect that their tissue concentrations remain approximately constant, while other FFAs concentrations are increased. The ratio

of unsaturated FAs to saturated FAs indicates the ability of zooxanthellae algae to endure thermal stress (Wada 1994; Tchernov et al. 2004) and polyunsaturated FAs have been found to decrease at higher temperatures in photosynthetic organisms (Marr and Ingraham 1962; Murakami et al. 2000; Falcone et al. 2004). This appears to be a result of lipid peroxidation, due to saturated FAs being less susceptible to peroxidation compared with PUFAs (Ramalho et al. 1998; Lesser 2006), and to preserve the host-membrane integrity (Hubert 2003; Imbs and Yakovleva 2012). We observed no significant change in the ratio of total unsaturated FAs to total saturated FAs in response to temperature (Fig. 6). The corals studied here did not appear stressed and exhibited calcification and photosynthetic rates that were comparable to those of field specimens (Cole et al. 2018).

Our observation that the contribution of unsaturated FFA C18:2 to total FFAs increases at higher temperature agrees

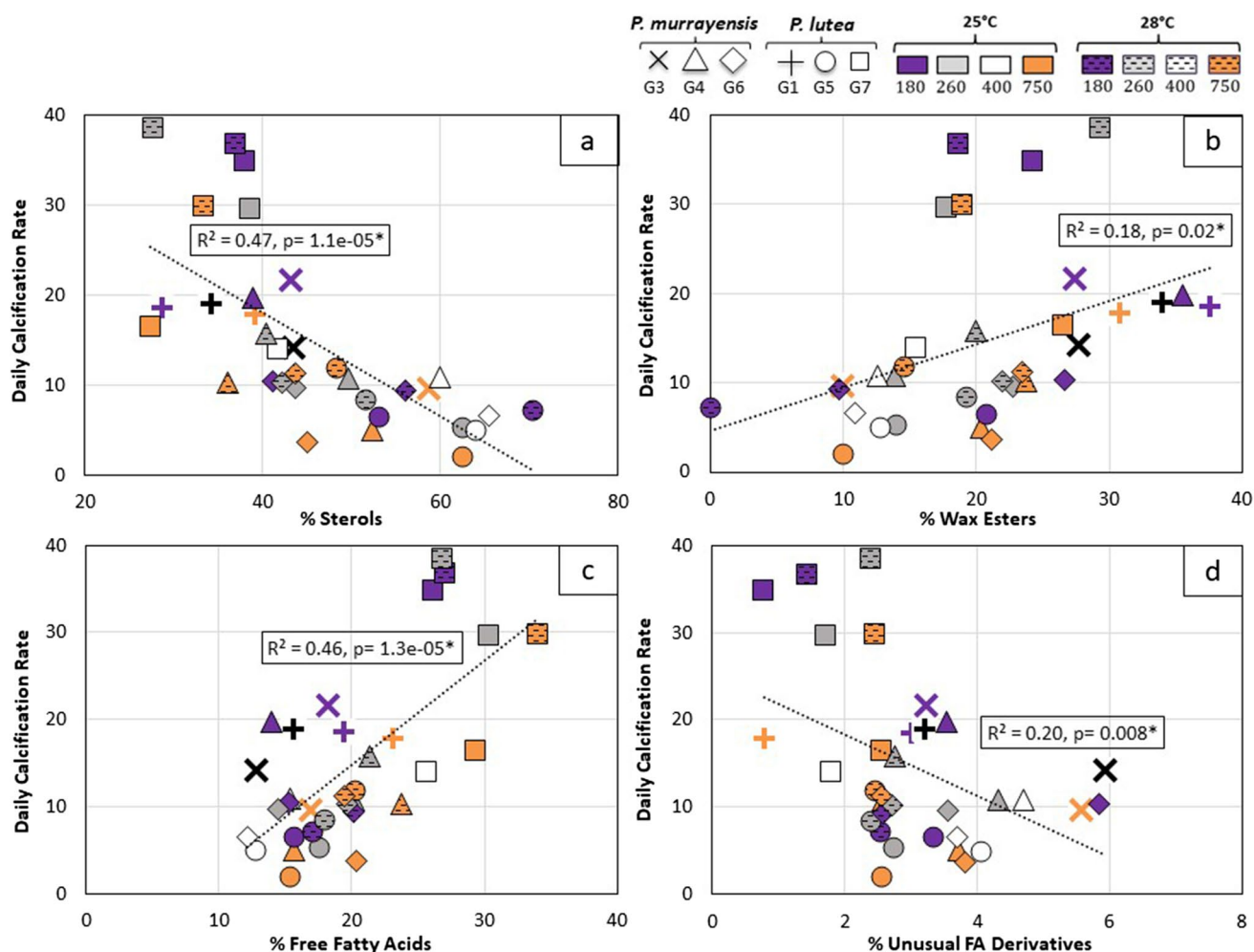


Fig. 7 Regression graphs for daily calcification rate ($\mu\text{mol CaCO}_3 \text{ cm}^{-2} \text{ d}^{-1}$) versus **a** %sterols **b** %wax Esters **c** %free fatty acids **d** %unusual FA derivatives, detected through GC–MS analysis within G1 and G3 *Porites* spp. genotypes cultured during experiment 1, as well as G4, G5, G6, G7 *Porites* spp. genotypes cultured during

experiment 2. Removing G7 from the datasets alters the coefficients of determination and p values for each graph to **a** $R^2=0.50$, $p=5.7\text{e-}05^*$; **b** $R^2=0.50$, $p=5.4\text{e-}05^*$; **c** $R^2=0.04$, $p=0.30$; and **d** $R^2=0.008$, $p=0.66$

with studies in other photosynthetic organisms, such as the *Arabidopsis* plant (Falcone et al. 2004), and suggests that this unsaturated FFA may be involved in acclimation to higher temperatures. Defined proportions of saturated and unsaturated fatty acids are required within membrane lipids to allow for photosynthetic thermostability and acclimation to higher temperature (Falcone et al. 2004). Polyunsaturated C18:2 and C18:3 are essential fatty acids which animals are unable to synthesise de novo (Latyshev et al. 1991; Bachok et al. 2006; Bell et al. 2007). C18:3 is concentrated in the symbiont fraction of the coral, while C18:2 predominantly occurs in the host (Imbs et al. 2014), implying that C18:3 is synthesised by the algae, while C18:2 is mainly derived from heterotrophy. The % contribution of C18:2 to coral total fatty acids is increased by heterotrophy (Tan and Johns

1991; Yu et al. 2021) and the C18:2 increase observed in our study could reflect increased feeding at higher temperatures.

Seawater $p\text{CO}_2$

We observe no significant variations in any of the lipids in response to seawater $p\text{CO}_2$, with the exception that the contribution of C14:0 to FAME is significantly higher in corals cultured at both 750 μatm and 260 μatm compared to 180 μatm . Myristic acid (C14:0) is incorporated within the phospholipid bilayer of cell membranes and acts as a lipid anchor binding to protein receptors responsible for triggering various cellular responses (Cox and Nelson 2005). Corals cultured at high seawater $p\text{CO}_2$ may catabolise tissue lipids to maintain calcification rates comparable to those of low seawater $p\text{CO}_2$ corals (Wall et al. 2017) although a

decrease in tissue lipid is not observed in all studies when corals (e.g. *Montipora monasteriata*) sustain calcification at high seawater pCO₂ (Schoepf et al. 2013). Overall, our results show that changes in seawater pCO₂ have relatively little effect on coral tissue lipids in *Porites* spp., where higher temperatures have been previously reported to buffer the negative effects of increased pCO₂ (Schoepf et al. 2013).

Effect of coral genotype and calcification rate

Genotype G7 was the fastest calcifying coral in all seawater pCO₂ and temperature treatments (Cole et al. 2018) and this genotype exhibits multiple significant differences in lipids composition compared to the other corals (Table 1). Given the mixotrophic nature of the coral organism, we note that different coral genotypes of the same species may have vastly different nutritional strategies (Fox et al. 2019). The PUFAs C18:2 and C18:3 make significantly smaller and greater contributions, respectively, to the total FFA pool of this genotype. C18:3 is characteristic of zooxanthellae corals (Latyshev 1991; Imbs et al. 2010) and predominantly found in the symbiont fraction, while C18:2 is primarily located in the host (Imbs et al. 2014). We did not monitor the feeding of the corals in this study and the pattern observed in G7 could reflect a shift towards a higher contribution of autotrophy (versus heterotrophy) to the lipid pool compared to the other genotypes. Although we note that both gross and net photosynthetic rates in G7 were comparable to other corals in the study (Cole et al. 2018). Organisms can convert C18:2 to C18:3, but not vice versa (Cerone and Smith 2022) and the G7 pattern could alternatively indicate a higher conversion of C18:2 to C18:3 in this coral. C18:3 increased in *Montipora digitata* at higher irradiance (Papina et al. 2007), suggesting photosynthesis may promote C18:3. However, C18:3 also increased at depth in *Stylophora pistillata* (Latyshev et al. 1991), suggesting the relationship between PUFA and photosynthesis is not straightforward.

Genotype G7 also has lower contributions of total sterols, total unusual fatty acid derivatives, C17:0 FFA, and hexadecan-2-one, and higher contributions of total FFAs, stigmasterol, and octadecanol, to their relative groups. The coral animal is unable to synthesise sterols (Baumgarten et al. 2015; Hambleton et al. 2019) and coral tissue sterols are largely derived from the algae hosted in the coral (Treignier et al. 2008). Genotype-dependent variations in sterol composition could reflect changes in the algal strains hosted in the coral (Treignier et al. 2008; Babcock-Adams et al. 2016). Reef-building corals show plasticity in their sterol acquisition, and symbiont-derived sterol variants can substitute for prey-derived forms (e.g. cholesterol) (Hambleton et al. 2019). The decrease in unusual fatty acid derivatives coupled with an increase in FFAs in the G7 genotype may

indicate catabolism of the derivatives to form an additional source of FFAs.

Coral calcification rate is positively related to the % contributions of wax esters and FFAs and negatively related to the % contributions of sterols and unusual fatty derivatives to lipids (Fig. 7). Coral genotype G7 has a different lipid composition compared to the other corals and if we remove this genotype from the dataset then significant relationships are only observed between calcification rate and % sterols and % wax esters. Lipids are important in coral biomineralisation as they can serve as an energy source to support the metabolic costs of calcification and may also be involved in the control of CaCO₃ precipitation, e.g. via Ca²⁺ binding (Isa and Okazaki 1987; Reggi et al. 2016). The exact roles of lipids in biomineralisation are unknown. Wax esters provide lipid storage in zooplankton (Lee et al. 2006), as well as in corals (Grottoli et al. 2004), and we hypothesise that high concentrations of these lipids in the coral tissues may support rapid calcification. Sterols are observed in the skeletal organic material (Farre et al. 2010) and a reduction in their contribution to tissue lipids at high calcification rates may reflect their consumption in biomineralisation.

It is unclear if the altered lipid compositions in coral G7 act to increase the calcification rate of this genotype or reflect other influences. FFAs and sterols, combined with PUFAs, represent the majority of membrane lipids (Boutry et al. 1979; Wada 1994; Yamashiro 1999; Tchernov et al. 2004; Sharma 2006; Hambleton et al. 2019) and act as important regulators of both coral metabolism and stress resistance (Ward 1995; Hulbert 2003). Although the most rapidly calcifying coral, genotype G7 exhibited pronounced abnormalities in skeletal morphology in response to reduced seawater pCO₂ (Allison et al. 2022), suggesting this coral may have a low stress resilience. Further work is required to define the roles of lipids in calcification and in susceptibility to climate change.

Relevance to a changing climate

Massive tropical corals, such as *Porites* spp. are important reef-builders and support rich and diverse ecosystems across the Indo-Pacific region. Whilst calcifying marine organisms are increasingly vulnerable to rising sea surface temperatures and ocean acidification, some studies have shown that massive poritid corals may be less sensitive to these changes than other coral species (Gleason 1993; Baird and Marshall 2002; van Woesik et al. 2011; Fabricius et al. 2011; Crook et al. 2012). High coral energy reserves and changes in the dominant *Symbiodiniaceae* endosymbiont were found to allow rapid acclimation of the *Porites divaricata* Caribbean coral to experimentally elevated seawater temperatures, whilst low energy reserves and a relatively static *Symbiodiniaceae* composition increased the susceptibility of *Porites*

astreoides to bleaching, thus affecting coral health (Grottoli et al. 2014). Some effects on lipid composition are observed with increasing seawater temperature in the present study. The largest changes in lipid composition are observed between *Porites* spp. genotypes, regardless of treatment. The corals exhibited a broad range of calcification rates in this study (Cole et al. 2018), and some of these variations are correlated with calcification rate suggesting potential roles of lipids in biomineralisation.

Overall, our findings illustrate that the largest changes in lipid compositions are observed between massive *Porites* spp. genotypes rather than between temperature or seawater pCO₂ treatments. However, interesting differences in saturated and unsaturated fatty acid compositions between temperature treatments are also found. Large variations in calcification rate can be observed between coral genotypes and these can exceed calcification variations in response to ocean acidification within coral genotypes (Cole et al. 2018). Further work is required to determine if rapidly calcifying corals are more or less resilient to environmental changes and to identify how this relates to the lipid profiles of individual corals.

Acknowledgements This work was supported by the UK Natural Environment Research Council (award NE/I022973/1).

Funding Natural Environment Research Council, NE/I022973/1, Nicola Allison.

Declarations

Conflict of interest All authors declare to have no conflict of interest.

Ethical approval All applicable international, national, and/or institutional guidelines for the care and use of animals were followed.

Open Access This article is licensed under a Creative Commons Attribution 4.0 International License, which permits use, sharing, adaptation, distribution and reproduction in any medium or format, as long as you give appropriate credit to the original author(s) and the source, provide a link to the Creative Commons licence, and indicate if changes were made. The images or other third party material in this article are included in the article's Creative Commons licence, unless indicated otherwise in a credit line to the material. If material is not included in the article's Creative Commons licence and your intended use is not permitted by statutory regulation or exceeds the permitted use, you will need to obtain permission directly from the copyright holder. To view a copy of this licence, visit <http://creativecommons.org/licenses/by/4.0/>.

References

- Abdul QA, Choi RJ, Jung HA, Choi JS (2016) Health benefit of fucosterol from marine algae: a review. *J Sci Food Agric* 96(6):1856–1866
- Al-Lihaibi SS (2007) Aldehyde and ketone compounds from marine hydrocoral identified by gas chromatography-mass spectrometry. *E J Nat Subst* 2:1–4
- Allison N, Ross P, Brasier A, Cieminska N, Lopez Martin N, Cole C, Hintz K, Finch AA (2022) Effects of seawater pCO₂ on the skeletal morphology of massive *Porites* spp. corals. *Mar Biol* 169:73
- Al-Moghrabi S, Allemand D, Couret JM, Jaubert J (1995) Fatty acids of the Scleractinian coral *Galaxea fascicularis*: effect of light and feeding. *J Comparat Biol B* 165:183–192
- Anthony KRN (2006) Enhanced energy status of corals on coastal, high-turbidity reefs. *Mar Ecol Prog Ser* 319:11–116
- Athenstaedt K, Daum G (2006) The life cycle of neutral lipids: synthesis, storage and degradation. *Cell Mol Life Sci* 63:1355–1369
- Babcock-Adams L, Minarro S, Fitt WK, Medeiros PM (2016) Assessing coral response to a severe bleaching event using multimolecular Biomarkers. American Geophysical Union, Washington DC, pp 54–2250
- Bachok Z, Mfilinge P, Tsuchiya M (2006) Characterization of fatty acid composition in healthy and bleached corals from Okinawa, Japan. *Coral Reefs* 25:545–554
- Baird AH, Marshall PA (2002) Mortality, growth and reproduction in scleractinian corals following bleaching on the great barrier reef. *Mar Ecol Prog Ser* 237:133–141
- Barry JP, Tyrrell T, Hansson L, Plattner GK, Gattuso JP (2011) Atmospheric CO₂ targets for ocean acidification perturbation experiments. In: Riebesell U, Fabry VJ, Hansson L, Gattuso JP (eds) Guide to best practices for ocean acidification research and data reporting. European Communities, Belgium
- Baumann J, Grottoli AG, Hughes AD, Matsui Y (2014) Photoautotrophic and heterotrophic carbon in bleached and non-bleached coral lipid acquisition and storage. *Mar Bio Ecol* 461:469–478
- Baumgarten S, Simakov O, Esharik LY, Liew YJ, Lehnert EM, Mitchell CT et al (2015) The genome of *Aiptasia*, a sea anemone model for coral symbiosis. *PNAS* 221(38):11893–11998
- Beck JG, Mathieu D, Loudet C, Buchoux S, Dufourc EJ (2007) Plant sterols in 'rafts': a better way to regulate membrane thermal shocks. *FASEB J* 21:1714–1723
- Bell MV, Dick JR, Anderson TR, Pond DW (2007) Application of liposome and stable isotope tracer techniques to study polyunsaturated fatty acid biosynthesis in marine zooplankton. *J Plankton Res* 29:417–422
- Bligh EG, Dyer WJ (1959) A rapid method of total lipid extraction and purification. *J Biochem Physiol* 37:911–917
- Boutry JL, Saliot A, Barbier M (1979) The diversity of marine sterols and the role of algal biomasses; from facts to hypothesis. *Experientia* 35:1541–1543
- Burton EA, Walter LM (1987) Relative precipitation rates of aragonite and Mg calcite from seawater: Temperature or carbonate ion control? *Geology* 15:111–114
- Carricart-Ganivet JP, Merino M (2001) Growth responses of the reef-building coral *Montastraea annularis* along a gradient of continental influence in the southern Gulf of Mexico. *Bull Mar Sci* 68:133–146
- Cerone M, Smith TK (2022) Desaturases: Structural and mechanistic insights into the biosynthesis of unsaturated fatty acids. *IUBMB Life* 74(11):1036–1051
- Chen HK, Rosset SL, Wang LH, Chen CS (2021) The characteristics of host lipid body biogenesis during coral-dinoflagellate endosymbiosis. *PeerJ* 9:e11652
- Clausen CD, Roth AA (1975) Effect of temperature and temperature adaptation on calcification rate in the hermatypic coral *Pocillopora damicornis*. *Mar Biol* 33:93–100
- Cole C, Finch A, Hintz C, Hintz K, Allison N (2016) Understanding cold bias: variable response of skeletal Sr/Ca to seawater pCO₂ in acclimated massive *Porites* corals. *Sci Rep* 6:26888

- Cole C, Finch A, Hintz C, Hintz K, Allison N (2018) Effects of seawater pCO₂ and temperature on calcification and productivity in the coral genus *porites* spp.: an exploration of potential interaction mechanisms. *Coral Reefs* 37:471–481
- Conlan JA, Rocker MM, Francis DS (2017) A comparison of two common sample preparation techniques for lipid and fatty acid analysis in three different coral morphotypes reveals quantitative and qualitative differences. *PeerJ* 5:e3645
- Coronado I, Fine M, Bosellini FR, Stolarski J (2019) Impact of ocean acidification on crystallographic vital effect of the coral skeleton. *Nat Commun* 10:1–9
- Cox DL, Nelson MM (2005) *Lehninger principles of biochemistry*, 4th edn. W.H Freeman, New York
- Crandall JB, Teece MA, Estes BA, Manfrino C, Ciesla JH (2016) Nutrient acquisition strategies in mesophotic hard corals using compound specific stable isotope analysis of sterols. *J Exp Mar Biol Ecol* 474:133–141
- Crook ED, Potts D, Rebolledo-Vieyra M, Hernandez L, Paytan A (2012) Calcifying coral abundance near low-pH springs: implications for future ocean acidification. *Coral Reefs* 31:239–245
- Doney SC, Fabry VJ, Feely RA, Kleypas JA (2009) Ocean acidification: the other CO₂ problem. *Annu Rev Mar Sci* 1:169–192
- Edmunds PJ, Burgess SC (2016) Size-dependent physiological responses of the branching coral *pocillopora verrucosa* to elevated temperature and pCO₂. *J Exp Biology* 291:3896–3906
- Fabricius KE, Langdon C, Uthicke S, Humphrey C, Noonan S, De'ath G, Okazaki R, Muehllehner N, Glas MS, Lough JM (2011) Losers and winners in coral reefs acclimatized to elevated carbon dioxide concentrations. *Nat Clim Change* 1:165–169
- Falcone DL, Ogas JP, Somerville CR (2004) Regulation of membrane fatty acid composition by temperature in mutants of *Arabidopsis* with alterations in membrane lipid composition. *BMC Plant Biol* 4:17
- Falini G, Fermani S, Goffredo S (2015) Coral biomineralization: A focus on intra-skeletal organic matrix and calcification. *Semin Cell Dev Biol* 46:17–26
- Farre B, Cuif JP, Dauphin Y (2010) Occurrence and diversity of lipids in modern coral skeletons. *Zoology (jena)* 113:250–257
- Forsman ZH, Barshis DJ, Hunter CL, Toonen RJ (2009) Shape-shifting corals: Molecular markers show morphology is evolutionarily plastic in *porites*. *BMC Evol Biol* 9:45
- Fox MD, Elliott Smith EA, Smith JE, Newsome SD (2019) Trophic plasticity in a common reef-building coral: insights from $\delta^{13}\text{C}$ analysis of essential amino acids. *Funct Ecol* 33:2203–2214
- Gleason MG (1993) Effects of disturbance on coral communities: bleaching in Moorea, French Polynesia. *Coral Reefs* 12:193–201
- Glynn PW, Perez M, Gilchrist SL (1985) Lipid decline in stressed corals and their crustacean symbionts. *Biol Bull* 168:276–284
- Goulet TL, Erill I, Ascunce MS, Finley SJ, Javan GT (2020) Conceptualization of the holobiont paradigm as it pertains to corals. *Front Physiol* 11:566968
- Grottoli AG, Rodrigues LJ, Juarez C (2004) Lipids and stable carbon isotopes in two species of Hawaiian corals, *Porites compressa* and *Montipora verrucosa*, following a bleaching event. *Mar Biol* 145:621–631
- Grottoli AG, Rodrigues LJ (2011) Bleached *Porites compressa* and *Montipora capitata* corals catabolize $\delta^{13}\text{C}$ -enriched lipids. *Coral Reefs* 30:687–692
- Grottoli AG, Warner ME, Levas SJ, Aschaffenburg MD, Schoepf V, McGinley M, Baumann J, Matsui Y (2014) The cumulative impact of annual coral bleaching can turn some coral species winners into losers. *Glob Chang Biol* 20:3823–3833
- Grottoli AG, Tchernov D, Winters G (2017) Physiological & Biogeochemical Responses of Super-Corals to Thermal Stress from the Northern Gulf of Aqaba. *Red Sea Front Mar Sci* 4:215
- Hambleton EA, Shivas VA, Maegele JI, Kvaskoff D, Sachsenheimer T, Guse A (2019) Sterol transfer by atypical cholesterol-binding NPC2 proteins in coral-algal symbiosis. *Elife* 8:e43923
- Harland AD, Fixter LM, Spencer Davies P, Anderson RA (1991) Distribution of lipids between the zooxanthellae and animal compartment in the symbiotic sea anemone *Anemonia viridis*: wax esters, triglycerides and fatty acids. *Mar Biology* 110:13–19
- Harland AD, Navarro JC, Spencer Davies P, Fixter LM (1993) Lipids of some caribbean and red sea corals: total lipid, wax esters, triglycerides and fatty acids. *Mar Biol* 117:113–117
- Hoegh-Guldberg O, Mumby PJ, Hooten AJ, Steneck RS, Greenfield P, Gomez E, Harvell CD, Sale PF, Edwards AJ, Caldeira K, Knowlton N, Eakin CM, Iglesias-Prieto R, Muthiga N, Bradbury RH, Dubi A, Hatzitolos ME (2007) Coral reefs under rapid climate change and ocean acidification. *Science* 318:1737–1742
- Hulbert AJ (2003) Life, death and membrane bilayers. *J Exp Biology* 206(14):2303–2311
- Ichihara K, Fukubayashi Y (2010) Preparation of the fatty acid methyl esters for gas-liquid chromatography. *J Lipid Res* 51(3):635–640
- Imbs AB, Latyshev NA, Dautova TN, Latypov YY (2010) Distribution of lipids & fatty acids in corals by their taxonomic position and presence of zooxanthellae. *Mar Ecol Progr Ser* 409:55–65
- Imbs AB, Yakovleva IM (2012) Dynamics of lipid and fatty acid composition of shallow water corals under thermal stress: an experimental approach. *Coral Reefs* 31:41–53
- Imbs AB (2013) Fatty acids and other lipids of corals: composition, distribution, and biosynthesis. *Russ J Mar Biol* 39(3):153–168
- Imbs AB, Yakovleva IM, Dautova TN, Bui LH, Jones P (2014) Diversity of fatty acid composition of symbiotic dinoflagellates in corals: evidence for the transfer of host PUFAs to the symbionts. *Phytochemistry* 101:76–82
- Isa Y, Okazaki M (1987) Some observations on the Ca²⁺-binding phospholipid from scleractinian coral skeletons. *Comp Biochem Physiol B* 87:507–512
- Kaneda T (1991) Iso- and anteiso-fatty acids in bacteria: biosynthesis, function, and taxonomic significance. *Microbiol Rev* 55:288–302
- Latyshev N, Naumenko N, Svetashev V, Latypov Y (1991) Fatty acids of reef-building corals. *Mar Ecol Progr Ser* 76:295–301
- Leal MC, Nejstgaard JC, Calado R, Thompson ME, Frischer ME (2014) Molecular assessment of heterotrophy and prey digestion in zooxanthellate cnidarians. *Mol Ecol* 23:3838–3848
- Le Campion-Alsumard T, Golubic S, Hutchings P (1995a) Microbial endoliths in skeletons of live and dead corals: *Porites lobata* (Moorea, French Polynesia). *Mar Ecol Progr Ser* 117:149–157
- Le Campion-Alsumard T, Golubic S, Priess K (1995b) Fungi in corals: symbiosis or disease? Interaction between polyps and fungi causes pearl-like skeleton biomineralisation. *Mar Ecol Progr Ser* 117:137–147
- Lee RF, Hagen W, Kattner G (2006) Lipid storage in marine zooplankton. *Mar Ecol Progr Ser* 307:273–306
- Lee J, Jeon J, Yim MJ, Choi G, Lee MS, Park YG, Lee DS (2020) Comparison of fucosterol content in algae using high-performance liquid chromatography. *Fish Aquatic Sci* 23:9
- Lesser MP (2006) Oxidative stress in marine environments: Biochemistry and physiological ecology. *Annu Rev Physiol* 68:253–278
- Marr AG, Ingraham JL (1962) Effect of temperature on the composition of fatty acids in *Escherichia coli*. *J Bacteriol* 84(6):1260–1267
- Marubini F, Barnett H, Langdon C, Atkinson MJ (2001) Dependence of calcification on light and carbonate ion concentration for the hermatypic coral *Porites compressa*. *Mar Ecol Progr Ser* 220:153–162
- Mehdinia A, Sheijooni Fumani N, Saleh A, Vajed Samiei J, Seyed Hashtroudi M (2015) Seasonal changes in the content and composition of lipids in *Acropora downingi*. *J Persian Gulf (mar Sci)* 6:1–8

- Mollica NR, Guo W, Cohen AL, Huang KF, Foster GL, Donald HK, Solow AR (2018) Ocean acidification affects corals growth by reducing skeletal density. *PNAS* 115(8):1754–1759
- Murakami Y, Tsuyama M, Kobayashi Y, Kodama H, Iba K (2000) Trienoic fatty acids and plant tolerance of high temperature. *Science* 287(5452):476–479
- Muscantine L (1990) The role of symbiotic algae in carbon and energy flux in reef corals. *Ecosyst World* 25:75–87
- Oku H, Yamashiro H, Onaga K, Sakai K, Iwasaki H (2003) Seasonal changes in the content and composition of lipids in the coral *Goniastrea aspera*. *Coral Reefs* 22:83–85
- Pandolfi JM, Connolly SR, Marshall DJ, Cohen AL (2011) Projecting coral reef futures under global warming and ocean acidification. *Science* 333:418–422
- Papina M, Meziane T, Van Woesik R (2003) Symbiotic zooxanthellae provide the host-coral *Montipora digitata* with polyunsaturated fatty acids. *Comp Biochem Physiol B Biochem Mol Biol* 135:533–537
- Papina M, Meziane T, van Woesik R (2007) Acclimation effect on fatty acids of the coral *Montipora digitata* and its symbiotic algae. *Comp Biochem Physiol B Biochem Mol Biol* 147(4):583–589
- Patton JS, Abraham S, Benson AA (1977) Lipogenesis in the intact coral *Pocillopora capitata* and its isolated zooxanthellae: evidence for a light-driven carbon cycle between symbiont and host. *Mar Biol* 44:235–247
- Pichon M (2011) Porites. In: Hopley D (ed) *Encyclopedia of modern coral reefs*. encyclopedia of earth sciences series. Springer, Dordrecht
- Ramvalho JC, Campos PS, Teixeira M, Nunes MA (1998) Nitrogen dependent changes in antioxidant system and in fatty acid composition of chloroplast membranes from *Cofea arabica* L. plants submitted to high irradiance. *Plant Sci* 135:115–124
- Reggi M, Fermani S, Samori C, Gizzi F, Prada F, Dubinsky Z, Goffredo S, Falini G (2016) Influence of intra-skeletal coral lipids on CaCO₃ precipitation. *Cryst Eng Comm* 18:8829–8833
- Samori C, Caroselli E, Prada F, Reggi M, Fermani S, Dubinsky Z, Goffredo S, Falini G (2017) Ecological relevance of skeletal fatty acid concentration and composition in Mediterranean scleractinian corals. *Sci Rep* 7:1929
- Schoepf V, Grottoli AG, Warner ME, Cai WJ, Melman TF, Hoadley KD, Tye Pettay D, Hu X, Li Q, Xu H, Wang Y, Matsui Y, Baumann JH (2013) Coral energy reserves and calcification in a high CO₂ world at two temperatures. *PLoS ONE* 8:e75049
- Seemann J, Sawall Y, Auel H, Richter C (2012) The use of lipids and fatty acids to measure the trophic plasticity of the coral *Stylophora subseriata*. *Lipids* 48:275–286
- Sharma SC (2006) Implications of sterol structure for membrane lipid composition, fluidity and phospholipid asymmetry in *Saccharomyces cerevisiae*. *FEMS Yeast Res* 6(7):1047–1051
- Spencer Davies P (1991) Effect of daylight variations on the energy budgets of shallow-water corals. *Mar Biol* 108:137–144
- Tambutté E, Venn A, Holcomb M, Segonds N, Techer N, Zoccola D, Allemand D, Tambutté S (2015) Morphological plasticity of the coral skeleton under CO₂-driven seawater acidification. *Nat Commun* 6:7368
- Tan CK, Johns MR (1991) Fatty acid production by heterotrophic *Chlorella saccharophila*. *Hydrobiologia* 215:13–19
- Tchernov D, Gorbunov MY, de Vargas C, Yadav SN, Milligan AN, Häggblom M, Falkowski PG (2004) Membrane lipids of symbiotic algae are diagnostic of sensitivity to thermal bleaching in corals. *Proc Natl Acad Sci USA* 101:13531–13535
- Teece MA, Estes B, Gelsleichter E, Lirman D (2011) Heterotrophic and autotrophic assimilation of fatty acids by two scleractinian corals, *Montastraea faveolata* and *Porites astreoides*. *Limnol Oceanogr* 56(4):1285–1296
- Tolosa I, Treignier C, Grover R, Ferrier-Pagès C (2011) Impact of feeding and short-term temperature stress on the content and isotopic signature of fatty acids, sterols, and alcohols in the Scleractinian coral *Turbinaria reniformis*. *Coral Reefs* 30:764–774
- Treignier C, Grover R, Ferrier-Pagès C, Tolosa I (2008) Effect of light and feeding on the fatty acid and sterol composition of zooxanthellae and host tissue isolated from the scleractinian coral *Turbinaria reniformis*. *Limnol Oceanogr* 53:2702–2710
- van Woesik R, Sakai K, Ganase A, Loya Y (2011) Revisiting the winners and the losers a decade after coral bleaching. *Mar Ecol Prog Ser* 434:67–76
- Veron JEN (2000) Corals of the world. In: Stafford-Smith MG (ed) *Australian institute of marine science*. Townsville
- Wada H (1994) Contribution of membrane lipids to the ability of the photosynthetic machinery to tolerate temperature stress. *Proc Natl Acad Sci USA* 91:4273–4277
- Wall CB, Mason RAB, Ellis WR, Cuning R, Gates RD (2017) Elevated pCO₂ affects tissue biomass composition, but not calcification, in a reef coral under two light regimes. *R Soc Open Sci* 4:170683
- Ward S (1995) Two patterns of energy allocation for growth, reproduction, and lipid storage in the scleractinians coral *Pocillopora damicornis*. *Coral Reefs* 14:87–90
- Yamashiro H, Oku H, Higa H, Chinen I, Sakai K (1999) Composition of lipids, fatty acids and sterols in Okinawan corals. *Comp Biochem Physiol B* 122:397–407
- Yu X, Jiang L, Gan J, Zhang Y, Luo Y, Liu C, Huang H (2021) Effects of feeding on production, body composition and fatty acid profile of scleractinian coral *Galaxea fascicularis*. *Aquac Rep* 21(100871):2352–5134

Publisher's Note Springer Nature remains neutral with regard to jurisdictional claims in published maps and institutional affiliations.